Post-fire changes in net shortwave radiation along a latitudinal gradient in boreal North America

Yufang Jin,[1] James T. Randerson,[1] Michael L. Goulden,[1] and Scott J. Goetz[2]

Received 23 March 2012; revised 8 June 2012; accepted 13 June 2012; published 14 July 2012.

[1] Understanding how a changing boreal fire regime is likely to influence regional climate requires detailed information about fire effects on the surface radiation budget. We used time series of satellite observations of surface albedo from 2000–2011 and fire perimeters since 1970 to study post-fire changes in surface net shortwave radiation along a latitudinal transect in central Canada. Fire-induced surface shortwave forcing (SSF) integrated over an annual cycle for the first 30 years after fire was similar (-4.1 W m^{-2} with a 95% confidence interval of -4.5 to -3.7 W m^{-2}) between southern and northern boreal regions. The lack of a latitudinal difference in SSF was caused by counteracting latitudinal trends in seasonal contributions. Spring (March, April, and May) SSF increased with latitude, from -7.2 W m^{-2} in the south to -10.1 W m^{-2} in the north, primarily because of delayed snow melt, which amplified albedo differences between unburned forests and recovering stands. In contrast, winter incoming solar radiation and summer albedo change decreased from south to north, resulting in a decreasing latitudinal trend in winter and summer SSF. Vegetation recovery was slower in the north, leading to smaller increases in summer albedo during the first decade after fire, and a prolonged phase of elevated spring albedo during the second decade. Our results indicate that fires reduce surface net shortwave radiation considerably for many boreal forest ecosystems in North America, providing further evidence that disturbance-mediated shifts in surface energy exchange need to be considered in efforts to manage these forests for climate change mitigation. **Citation:** Jin, Y., J. T. Randerson, M. L. Goulden, and S. J. Goetz (2012), Post-fire changes in net shortwave radiation along a latitudinal gradient in boreal North America, *Geophys. Res. Lett.*, *39*, L13403, doi:10.1029/2012GL051790.

1. Introduction

[2] Significant warming has occurred in the North American boreal region in recent decades [*Hinzman et al.*, 2005], resulting in changes in the fire regime [*Gillett et al.*, 2004; *Kasischke and Turetsky*, 2006] and reduced spring snow cover extent and duration [*Déry and Brown*, 2007; *Brown and Robinson*, 2011]. These trends are expected to continue or accelerate through the 21st century under the warmer and drier regional climate expected with climate change [*Flannigan et al.*, 2005; *Balshi et al.*, 2009; *Krawchuk and Cumming*, 2011]. Fire is a common and widespread disturbance agent in boreal forest that influences ecosystem structure and function in many ways [*McGuire et al.*, 2004; *Goetz et al.*, 2012]. Changes in the fire regime affect climate through several feedbacks [*Euskirchen et al.*, 2009], including changes in carbon exchange [*Bond-Lamberty et al.*, 2007; *Turetsky et al.*, 2011] and alteration of surface energy exchange [*Amiro et al.*, 2006; *Randerson et al.*, 2006; *Bond-Lamberty et al.*, 2009]. Fires also influence aerosol emissions and deposition, which, in turn, influence the climate system through effects on the atmospheric radiation budget and snow-albedo feedbacks [*Flanner et al.*, 2011]. Satellite observations have not been used to systematically characterize how fire-induced changes in albedo and surface net radiation vary with latitude or biome type. Understanding this heterogeneity is particularly important in boreal Canada, where climate, fire, and topography interact to create a patchwork of differing stand ages, species composition, and biophysical properties [*Amiro et al.*, 2006].

[3] Surface forcing, defined as the instantaneous radiative flux change at the surface, is a useful diagnostic for understanding the implications of land surface perturbation on climate [*Forster et al.*, 2007]. The surface shortwave forcing (SSF) associated with fire-induced changes in land cover is controlled by surface albedo changes ($\Delta\alpha$) and incoming solar radiation (S_{in}), both of which vary with latitude. Disturbance from fire changes leaf reflectance and also the three-dimensional structure of the forest canopy. Early successional plant functional types, such as grasses, shrubs, and broadleaf deciduous trees, are more reflective than evergreen needleleaf trees during the growing season [e.g., *Betts and Ball*, 1997]. They also have less of a masking effect on surface snow cover, resulting in higher albedo during fall, winter and spring $\Delta\alpha$ thus varies across boreal regions because of differences in species composition, canopy structure, patterns of succession, and duration and depth of snow cover. S_{in}, in contrast, is primarily controlled by earth-sun geometry and cloud cover.

[4] Latitudinal changes in tree density, from closed-canopy stands in the south to open woodlands in the north [*Timoney et al.*, 1993], may be expected to reduce post-fire albedo changes in northern regions because of a smaller absolute change in canopy structure [*Chambers et al.*, 2005]. The increase in snow season length from south to north, however, may counteract these structural effects, since post-fire albedo increases are largest during spring and fall when snow cover in recently burned stands is more exposed [*Liu et al.*, 2005]. Moreover, decreases in S_{in} from south to north should reduce SSF in more northern forests. Finally, the rate of post-fire vegetation recovery and regional differences in species composition during succession further

[1]Department of Earth System Science, University of California, Irvine, California, USA.
[2]Woods Hole Research Center, Falmouth, Massachusetts, USA.

Corresponding author: Y. Jin, Department of Earth System Science, University of California, Irvine, CA 92697, USA. (yufang@uci.edu)

0094-8276/12/2012GL051790

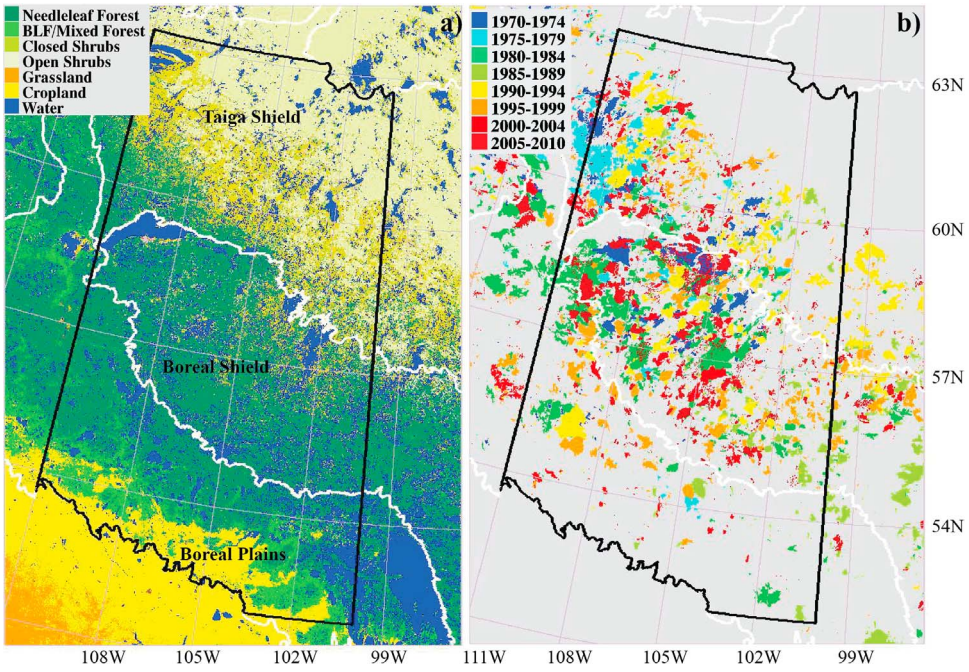

Figure 1. Boundaries of the transect area (in black) are superimposed on (a) vegetation types from the MODIS land cover product and (b) area burned during 1970–2010 in the central western Canada boreal region. Only fires greater than 100 ha were included in our analysis. Boundaries of boreal ecozones are shown in white. The majority of study areas are located in Saskatchewan and Northwest Territories, followed by Manitoba and Alberta.

complicate our ability to predict how SSF following fire varies with latitude [*Amiro et al.*, 2006; *Beck et al.*, 2011]. It is not clear how these factors trade off at various temporal and spatial scales for boreal forests in North America. A regional transect covering a large ecoclimatic gradient provides an effective means to investigate this question.

[5] *In situ* field studies have provided insight into the surface energy changes that occur following fire [*Chambers and Chapin*, 2002; *Liu et al.*, 2005; *Amiro et al.*, 2006; *Goulden et al.*, 2011], but these intensive chronosequence studies are necessarily limited in temporal and spatial coverage by the high cost of field work. The use of satellite remote sensing has permitted large-spatial-scale studies of fire-induced albedo change in Alaska [*Lyons et al.*, 2008; *Beck et al.*, 2011], but broader scale studies of different components of the surface energy budget are needed. Here we combine historical digital fire perimeter data and time series of satellite observations of surface albedo and vegetation dynamics to quantify how post-fire changes in surface albedo and SSF change as a function of latitude in boreal forest ecosystems. We focus our analysis on a north-south transect in central Canada and quantify the relative importance of the various factors that regulate the latitudinal variation in SSF.

2. Data and Methods

[6] We focused on a latitudinal transect between 52°N–63°N that encompassed three ecozones in central Canada (Figure 1). The study area was divided into three latitudinal zones from south to north based on the boundaries of the boreal plains, boreal shield, and taiga shield ecozones. This continuous transect crossed a pronounced ecoclimatic gradient. The climate is comparatively warm and dry in the south [*Price and Apps*, 1995]. Conditions are colder and drier in the north, where low winter temperatures are thought to limit the growth and reproduction of tree species [*Bonan and Shugart*, 1989]. A general gradient of decreasing soil fertility also occurs from south to north. Maximum site productivities generally occur in mid-boreal regions, presumably as a result of interactions between moisture, temperature and nutrient gradients [*Gower et al.*, 2001]. Vegetation across the region is dominated by needleleaf forests, with deciduous broadleaf stands more abundant in the south, and open forest stands with shrubs and lichen ground cover (taiga), more abundant in the north [*Marshall et al.*, 1999].

[7] We used the Canadian National Fire Database (Version 2011) produced by the Canadian Forest Service to identify the location and date of fires larger than 100 ha [*Amiro et al.*, 2001; *Stocks et al.*, 2003]. Digital fire perimeters were available since 1945 for Saskatchewan, since 1971 for the Northwest Territories, and since 1980 for Manitoba. In our analysis, we extracted fires that occurred from 1970 to 2010 and applied a 500 meter buffer within each polygon to reduce uncertainties in georegistration and fire perimeter delineation [after *Goetz et al.*, 2006] (Figure 1b). A total of 2232 fires (polygons) were analyzed, comprising a total burned area of 33.1 million ha (Table S1 of the auxiliary material).[1]

[8] We used the surface bidirectional reflectance distribution function (BRDF) and albedo products from Terra and Aqua MODIS observations (MCD43A1 and MCD43A3, collection 5) at 500 m resolution [*Schaaf et al.*, 2002], from March 2000 to December 2011. Shortwave albedo observations with the highest quality, as identified in the MODIS

[1]Auxiliary materials are available in the HTML. doi:10.1029/2012GL051790.

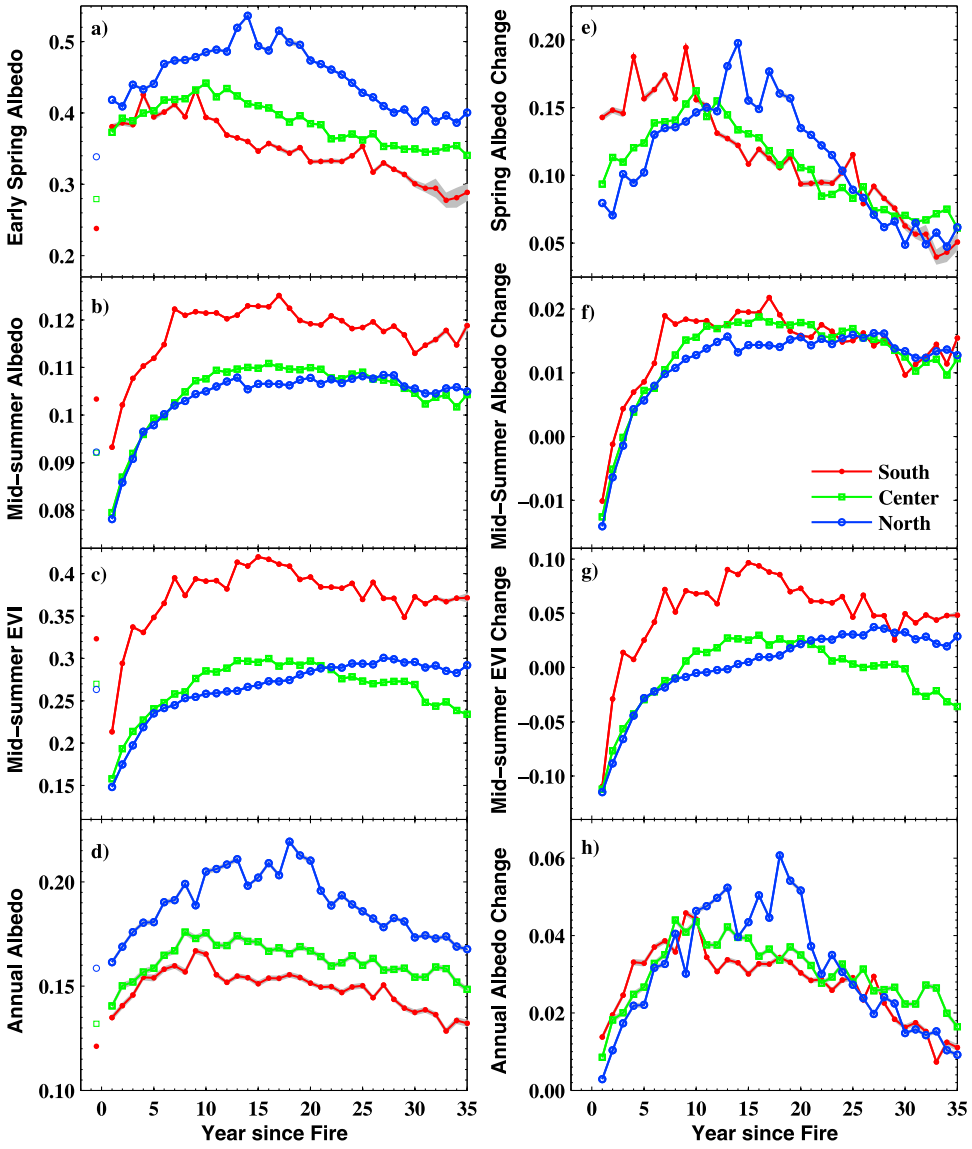

Figure 2. (a–d) Post-fire trajectories of shortwave albedos and EVI and of (e–h) their changes from pre-fire values as a function of year since fire. Mid-summer was here defined from DOY 177 to 224, and early spring was here defined from DOY 49 to 96. Gray areas represent 95% confidence intervals. Mean pre-fire values for each zone are represented in corresponding symbols before year 0 on X-axis.

quality product (MCD43A2) were extracted. We also used the 16-day enhanced vegetation index (EVI) product from Terra MODIS with a 500 m resolution (MOD13A1) [*Huete et al.*, 2002] to examine pre- and post-fire vegetation dynamics. Finally, we used the annual MODIS Land Cover product (MOD12Q1) [*Friedl et al.*, 2010] to identify the land cover types prior to fire and the vegetation composition in non-burned areas. Areas identified as water or wetland were excluded from our analysis. In boreal regions the accuracy of the collection 5 MODIS land cover product may be limited, particularly in the taiga shield where tree cover is sparse and MODIS classifies much of this area as shrubland.

[9] We developed a chronosequence of post-fire albedo and EVI for stands up to 40 years after fire by pooling the albedo observations from multiple burn perimeters for each zone. For example, the 2006 albedos for all areas that burned in 2004 were included in the pool of 2-year-old stands. We also constructed a pre-fire albedo climatology for each latitudinal zone by pooling all available pre-burn albedos within the perimeters of stands that burned in 2001–2010. For example, for a fire perimeter from 2010, we averaged all the albedo values from 2000–2009 for each 8-day interval. These observations were then averaged together with all the available pre-fire observations from other burn perimeters in the same transect belt (Figure S1 of the auxiliary material). We focused on the first 30 years after fire for our analysis of SSF since the digital fire perimeters were available since 1980 for all of the provinces within our study region.

[10] We calculated SSF based on the monthly mean all-sky incoming solar radiation at the surface (S_{in}) for 1983–2007 using the NASA Goddard Institute for Space Studies (GISS) solar radiation product. In the GISS product, S_{in} is computed using the GISS radiative transfer model driven by improved International Satellite Cloud Climatology Project-D series

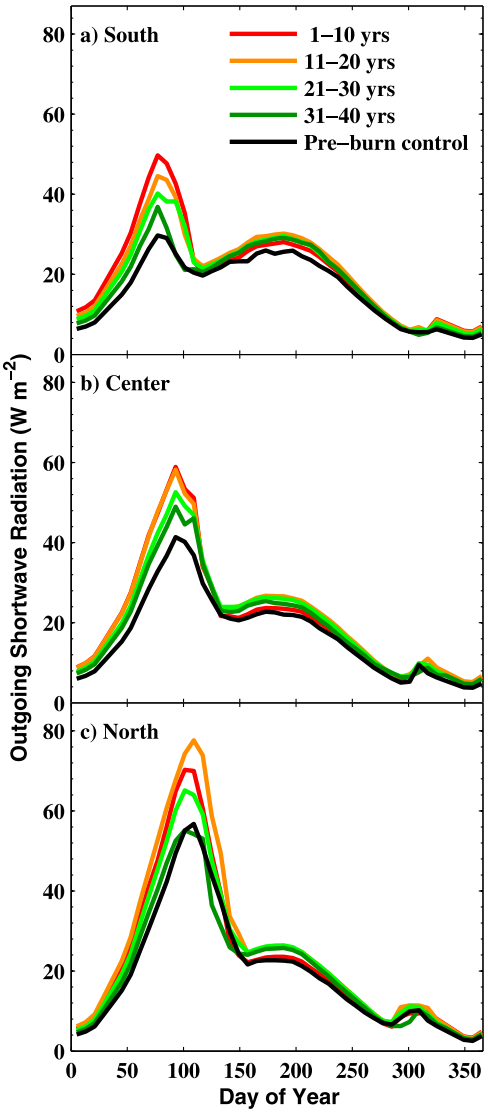

Figure 3. Outgoing shortwave radiation (S_{out}) for the pre-burn control and averaged over every 10 years after fire for each latitudinal zone in the study transect.

input data and is produced at 280 km resolution [*Zhang et al.*, 2004].

3. Results

3.1. Vegetation Recovery Patterns

[11] Analysis of the MODIS land cover product indicated that needleleaf forests accounted for 67% of the area burned during 2002–2011 in the southern zone. These forests also were the dominant plant functional type that burned in the central zone, accounting for 57% of the burned area. Closed shrublands accounted for 68% of the burned area in the northern zone (Table S2 of the auxiliary material). For unburned areas, the cover of needleleaf forests increased from 52°N to 57°N and then declined at higher latitudes (Figure S2 of the auxiliary material). In contrast, shrublands increased uniformly from south to north, and comprised approximately 88% of unburned land cover in the northernmost zone.

[12] Differences in pre-fire ecosystem structure and vegetation succession dominated the patterns of albedo change across the transect during the first two decades after fire (Figure 2). The southern zone had the lowest albedo in early spring (DOY 49–96) and highest albedo and EVI values in mid-summer (DOY 177–224) after fire (Figures 2a–2c). This zone also experienced the most rapid rate of post-fire vegetation recovery, e.g., EVI and mid-summer albedo exceeded pre-fire values 3 years after fire. Summer albedo change in the first two decades was consistently higher in the southern zone than in the other zones (Figure 2f). In early spring, the southern zone had the largest initial albedo increase (0.16 ± 0.06) until 9 years after fire, but decreased faster afterwards than other zones (Figure 2e). In the northern zone, the initial albedo increase in early spring was consistently the smallest (0.11 ± 0.06) for the first decade, mostly due to its higher pre-fire albedo values (Figure 2). Perhaps in response to slower rates of shrub and tree growth, as indicated by slower rates of EVI recovery, early spring albedo increases peaked much later in the northern zone, around 14 years after fire, and stayed higher in the northern zone than in the southern and central zones until 23 years after fire. As a result, the northern zone had much larger post-fire early spring albedo increases (0.16 ± 0.06) during the second decade. The central and northern zones had similar mid-summer EVI and albedo for the first 8 years after fire, but diverged around 10 years after fire with larger summer albedo and EVI change in the central zone. When integrated over an annual cycle, the increase in post-fire albedo decreased across the transect from 0.03 in the south to 0.02 in the north during the first decade, increased from 0.03 to 0.05 during the second decade, and was similar 0.03 during the third decade (Figure 2h and Table S3 of the auxiliary material). The 95% confidence intervals (CI) for all these albedo changes were approximately 0.001, and the annual mean was constructed by weighting each 16-day albedo by S_{in}.

3.2. Spring Contribution to Latitudinal Differences in SSF

[13] Spring albedo contributed the most to the annual outgoing shortwave radiation (S_{out}) in all zones, and its relative importance increased from south to north for both pre-fire and post-fire annual albedo and S_{out} (Figure 3 and Figure S3 of the auxiliary material). Northern regions had longer snow duration (Figure S4 of the auxiliary material) and thus longer time periods of sustained higher spring albedo (Figures S1 and S3 of the auxiliary material). The spring (March, April, and May) contribution to the annual pre-fire S_{out} increased from 36% in the southern zone to 52% in the northern zone, whereas the summer (June, July, and August) contribution decreased from 36% to 26%. Fall and winter together (September through February) contributed only approximately 28% to annual pre-fire S_{out} in the southern zone and 22% in the northern zone. Increases in the snow season length from south to north amplified latitudinal gradients of spring albedo before and after fire. Pre-fire spring albedo increased by about 82% along the transect, from 0.14 in the southern zone to 0.26 in the northern zone, while winter (December, January, February) albedo increased by only about 45%, from 0.22 to 0.32 (Table S3 of the auxiliary material). According to the snow cover flags in the MODIS albedo product, snow melting started earlier in the south in unburned areas, e.g., on DOY 90 in the southern zone as

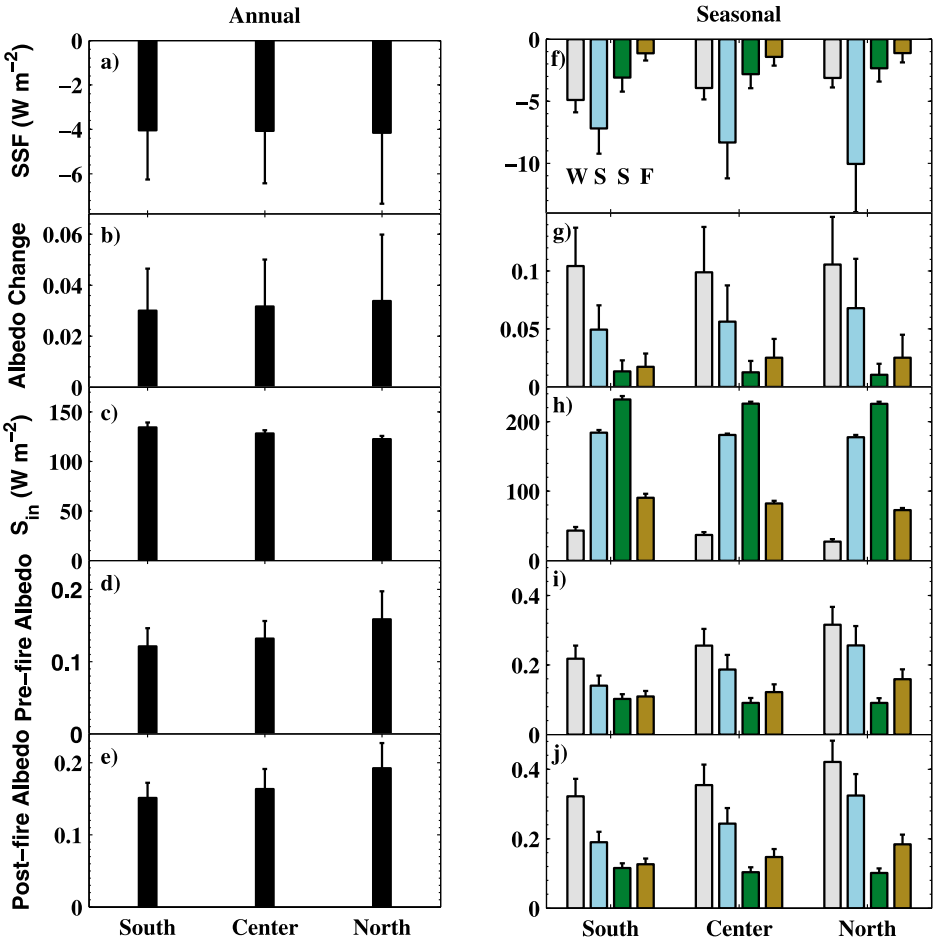

Figure 4. Latitudinal variations in mean annual (a) surface shortwave forcing (SSF), (b) post-fire albedo change, (c) incoming solar radiation (S_{in}), (d) pre-fire and (e) post-fire albedo averaged over the first 30 years after fire, and (f–j) the corresponding seasonal (winter, spring, summer, and fall) contributions. The albedo and the albedo changes during each 16-day period were weighted by S_{in} to obtain the annual mean and seasonal values. Error bars represent ±1 standard deviation.

compared to DOY 135 in the northern zone, and advancing by about 18 days per belt (Figure S4 of the auxiliary material). Similarly, snow accumulation began later in fall in the south, and the fall albedo (September, October, and November) decreased from 0.16 in the northern zone to 0.11 in the southern zone.

3.3. Regulation of Annual Mean SSF Across the Transect

[14] We found similar mean annual surface shortwave forcing along the north-south transect when averaged over the first 3 decades after fire for each chronosequence (Figure 4a). SSF was −4.1 W m^{-2} over the burned areas across all zones with a 95% CI of −4.5 to −3.7 W m^{-2}. The northern zone had the largest average annual albedo increase (0.034), 13% (95% CI, 9%–17%) higher than that in the southern zone (0.030) (Figure 4b and Table S3 of the auxiliary material). This was mostly offset by the decrease of mean annual S_{in} by 9% (±5%) from 134 ± 4.9 W m^{-2} in the southern zone to 123 ± 3.2 W m^{-2} in the northern zone (Figure 4c).

[15] Opposing trends of seasonal SSFs with latitude contributed to the overall lack of a latitudinal trend in the annual mean. Larger spring albedo changes and SSF in the northern zones were counteracted by relatively larger winter and summer SSFs in the southern zone (Figures 4f and 4g and Table S3 of the auxiliary material). When integrated over 30 years after fire, increases in spring albedo (approximately 0.07) were much larger (by 39%) in the northern zone than in the southern zones (0.05), resulting in a larger spring SSF by 40% (95% CI, 33%–47%) in the north (−10.1 W m^{-2}) than in the south (−7.2 W m^{-2}) (Figure 4g and Table S3 of the auxiliary material). Spring S_{in} decreased by only 3% in the northern zone compared with the southern zone. In contrast, winter S_{in} decreased by about 15 W m^{-2} (54%) from the southern to northern zone (Figure 4h), and winter albedo change increased only slightly from 0.10 in the south to 0.11 in the north. This resulted in a decreasing trend of winter SSF by 58% (95% CI, 27%–89%) with latitude (−4.9 vs. −3.1 W m^{-2}). In summer, the largest albedo change in the southern zone (0.013) produced the largest SSF (−3.1 W m^{-2}) as compared to −2.3 W m^{-2} in the north.

4. Discussion

[16] Our regional estimate of SSF averaged over the first 3 decades post-fire was within the range of previous estimates

(-3.0 to -6.2 W m^{-2}) derived from satellite observations of interior Alaska [*Lyons et al.*, 2008], even though our transect spanned several biomes and was further south. The maximum post-fire albedo increases and annual mean SSF we observed occurred during the second decade after fire. These results were consistent with *in situ* measurements from a Canadian boreal forest chronosequence [*McMillan and Goulden*, 2008]. The peak in negative forcing during the second decade may be attributable to several factors related to species succession after fire [*Serbin et al.*, 2009; *Goulden et al.*, 2011; *Alexander et al.*, 2012]. Deciduous herb and shrub cover, which is especially reflective in the near-infrared, typically increases during the first two decades and probably accounts for the initial increase in summer albedo [e.g., *Betts and Ball*, 1997]. Moreover, growth of deciduous trees substantially increases canopy height after the first decade post-fire [*Goetz et al.*, 2010], which in turn reduces the exposure of snow surfaces, and probably is a driver of the multi-decadal decline in early spring albedo we observed after 10–18 years in our study.

[17] Annual mean SSF averaged across the transect was smaller than an estimate from tower-based measurements for an individual fire in a black spruce forest (-11.2 W m^{-2}, *Randerson et al.* [2006]). Aside from the obvious spatial scale differences, this observation may be caused by several factors. Needleleaf forests accounted for only 57% to 67% of the total areas burned in the southern two zones during 2002–2010 (Table S2 of the auxiliary material) whereas this plant functional type accounted for more than 90% of the overstory canopy in the mature control stand in the *Randerson et al.* [2006] study. In addition, the MODIS mean pre-fire summer albedo (0.09 ± 0.01) and pre-snowmelt spring albedo (0.26 ± 0.06 to 0.29 ± 0.08 in the southern two zones) were higher than the mean of tower-based values of mature conifer stands across Canada and Alaska [e.g., *Amiro et al.*, 2006]. This suggests that by averaging within burn perimeters, stands with lower tree densities and more open canopies were included in our analysis, which are likely to have smaller post-fire increases in surface albedo as compared to denser and more homogeneous conifer stands that dominated the eddy covariance chronosequence studies.

[18] Considered together with other work on surface albedo in boreal forests across Canada and Alaska [e.g., *Amiro et al.*, 2006; *O'Halloran et al.*, 2012], our results provide evidence that a significant negative surface shortwave forcing due to fire-induced albedo change exists across many boreal forest ecosystems in North America. The negative radiative forcing documented here appears to be one of the key drivers of the observed decreases in surface temperature caused by disturbance in boreal regions [*Lee et al.*, 2011]. Our findings also highlight the importance of vegetation succession and snow cover duration in modulating the latitudinal patterns of annual albedo change and SSF averaged over the decades following fire. One important direction for future work is to investigate regional climate effects caused by SSF and other related changes in surface energy exchange, such as the magnitude and partitioning of sensible and latent heat and their impact on regional cloud cover. New findings on carbon emissions from fire disturbance [*Turetsky et al.*, 2011], surface temperature changes associated with forest removal [*Lee et al.*, 2011], and snow cover change due to fire-emitted carbonaceous particles [*Flanner et al.*, 2009] provide the foundation for a more comprehensive analysis of how forest and fire management strategies [e.g., *Anderson et al.*, 2011; *Carlson et al.*, 2010] may also influence radiative forcing and regional climate feedbacks across the boreal biome.

[19] **Acknowledgments.** The fire polygons were kindly provided by Canadian Forest Service. This work was supported by NASA grants NNX08AR69G (to Y.J.), NNX10AL14G (to Y.J., J.T.R., and M.L.G.), and NNX08AG13G (to S.J.G. and J.T.R.) as well as NOAA Global Carbon Cycle program (NA08OAR4310526 to S.J.G.) and NSF Office of Polar Programs (0732954 to S.J.G.). We thank W. Knorr, E. Kasischke, and one anonymous reviewer for their valuable comments.

[20] The Editor thanks Eric Kasischke and anonymous reviewer for their assistance in evaluating this paper.

References

Alexander, H., et al. (2012), Aboveground carbon accumulation across alternative post-fire successional trajectories within Alaskan boreal forests, *Ecosphere*, *3*(5), 1–21, doi:10.1890/ES11-00364.1.

Amiro, B. D., et al. (2001), Fire, climate change, carbon and fuel management in the Canadian boreal forest, *Int. J. Wildland Fire*, *10*(4), 405–413, doi:10.1071/WF01038.

Amiro, B. D., et al. (2006), The effect of post-fire stand age on the boreal forest energy balance, *Agric. For. Meteorol.*, *140*(1-4), 41–50, doi:10.1016/j.agrformet.2006.02.014.

Anderson, R. G., et al. (2011), Biophysical considerations in forestry for climate protection, *Front. Ecol. Environ*, *9*(3), 174–182, doi:10.1890/090179.

Balshi, M. S., et al. (2009), Assessing the response of area burned to changing climate in western boreal North America using a Multivariate Adaptive Regression Splines (MARS) approach, *Global Change Biol.*, *15*(3), 578–600, doi:10.1111/j.1365-2486.2008.01679.x.

Beck, P. S. A., et al. (2011), The impacts and implications of an intensifying fire regime on Alaskan boreal forest composition and albedo, *Global Change Biol.*, *17*(9), 2853–2866, doi:10.1111/j.1365-2486.2011.02412.x.

Betts, A. K., and J. H. Ball (1997), Albedo over the boreal forest, *J. Geophys. Res.*, *102*(D24), 28,901–28,909, doi:10.1029/96JD03876.

Bonan, G. B., and H. H. Shugart (1989), Environmental factors and ecological processes in boreal forests, *Annu. Rev. Ecol. Syst*, *20*, 1–28.

Bond-Lamberty, B., et al. (2007), Fire as the dominant driver of central Canadian boreal forest carbon balance, *Nature*, *450*(7166), 89–92, doi:10.1038/nature06272.

Bond-Lamberty, B., et al. (2009), Effects of fire on regional evapotranspiration in the central Canadian boreal forest, *Global Change Biol.*, *15*(5), 1242–1254, doi:10.1111/j.1365-2486.2008.01776.x.

Brown, R. D., and D. A. Robinson (2011), Northern Hemisphere spring snow cover variability and change over 1922–2010 including an assessment of uncertainty, *Cryosphere*, *5*(1), 219–229, doi:10.5194/tc-5-219-2011.

Carlson, M., et al. (2010), Maintaining the role of Canada's forests and peatlands in climate regulation, *For. Chron.*, *86*(4), 434–443.

Chambers, S. D., and F. S. Chapin (2002), Fire effects on surface-atmosphere energy exchange in Alaskan black spruce ecosystems: Implications for feedbacks to regional climate, *J. Geophys. Res.*, *108*(D1), 8145, doi:10.1029/2001JD000530.

Chambers, S. D., J. Beringer, J. T. Randerson, and F. S. Chapin III (2005), Fire effects on net radiation and energy partitioning: Contrasting responses of tundra and boreal forest ecosystems, *J. Geophys. Res.*, *110*, D09106, doi:10.1029/2004JD005299.

Déry, S. J., and R. D. Brown (2007), Recent Northern Hemisphere snow cover extent trends and implications for the snow-albedo feedback, *Geophys. Res. Lett.*, *34*, L22504, doi:10.1029/2007GL031474.

Euskirchen, E. S., A. D. McGuire, T. S. Rupp, F. S. Chapin III, and J. E. Walsh (2009), Projected changes in atmospheric heating due to changes in fire disturbance and the snow season in the western Arctic, 2003–2100, *J. Geophys. Res.*, *114*, G04022, doi:10.1029/2009JG001095.

Flanner, M. G., et al. (2009), Springtime warming and reduced snow cover from carbonaceous particles, *Atmos. Chem. Phys.*, *9*(7), 2481–2497, doi:10.5194/acp-9-2481-2009.

Flanner, M. G., et al. (2011), Radiative forcing and albedo feedback from the Northern Hemisphere cryosphere between 1979 and 2008, *Nat. Geosci.*, *4*(3), 151–155, doi:10.1038/ngeo1062.

Flannigan, M. D., et al. (2005), Future area burned in Canada, *Clim. Change*, *72*(1-2), 1–16, doi:10.1007/s10584-005-5935-y.

Forster, P. et al. (2007), Changes in atmospheric constituents and in radiative forcing, in *Climate Change 2007: The Physical Science Basis, Contribution of Working Group I to the Fourth Assessment Report of the Intergovernmental Panel on Climate Change*, edited by S. Solomon et al., pp. 193–234, Cambridge Univ. Press, Cambridge, U. K.

Friedl, M. A., et al. (2010), MODIS Collection 5 global land cover: Algorithm refinements and characterization of new datasets, *Remote Sens. Environ.*, *114*(1), 168–182, doi:10.1016/j.rse.2009.08.016.

Gillett, N. P., A. J. Weaver, F. W. Zwiers, and M. D. Flannigan (2004), Detecting the effect of climate change on Canadian forest fires, *Geophys. Res. Lett.*, *31*, L18211, doi:10.1029/2004GL020876.

Goetz, S. J., G. Fiske, and A. Bunn (2006), Using satellite time series data sets to analyze fire disturbance and recovery in the Canadian boreal forest, *Remote Sens. Environ.*, *101*(3), 352–365, doi:10.1016/j.rse.2006.01.011.

Goetz, S. J., M. Sun, A. Baccini, and P. S. A. Beck (2010), Synergistic use of spaceborne lidar and optical imagery for assessing forest disturbance: An Alaska case study, *J. Geophys. Res.*, *115*, G00E07, doi:10.1029/2008JG000898.

Goetz, S. J., et al. (2012), Observations and assessment of forest carbon recovery following disturbance in North America, *J. Geophys. Res.*, *117*, G02022, doi:10.1029/2011JG001733.

Goulden, M. L., et al. (2011), Patterns of NPP, GPP, respiration, and NEP during boreal forest succession, *Global Change Biol.*, *17*(2), 855–871, doi:10.1111/j.1365-2486.2010.02274.x.

Gower, S. T., et al. (2001), Net primary production and carbon allocation patterns of boreal forest ecosystems, *Ecol. Appl.*, *11*(5), 1395–1411, doi:10.1890/1051-0761(2001)011[1395:NPPACA]2.0.CO;2.

Hinzman, L. D., et al. (2005), Evidence and implications of recent climate change in northern Alaska and other arctic regions, *Clim. Change*, *72*(3), 251–298, doi:10.1007/S10584-005-5352-2.

Huete, A., et al. (2002), Overview of the radiometric and biophysical performance of the MODIS vegetation indices, *Remote Sens. Environ.*, *83*(1-2), 195–213, doi:10.1016/S0034-4257(02)00096-2.

Kasischke, E. S., and M. R. Turetsky (2006), Recent changes in the fire regime across the North American boreal region—Spatial and temporal patterns of burning across Canada and Alaska, *Geophys. Res. Lett.*, *33*, L09703, doi:10.1029/2006GL025677.

Krawchuk, M. A., and S. G. Cumming (2011), Effects of biotic feedback and harvest management on boreal forest fire activity under climate change, *Ecol. Appl.*, *21*(1), 122–136, doi:10.1890/09-2004.1.

Lee, X., et al. (2011), Observed increase in local cooling effect of deforestation at higher latitudes, *Nature*, *479*, 384–387, doi:10.1038/nature10588.

Liu, H., J. T. Randerson, J. Lindfors, and F. S. Chapin III (2005), Changes in the surface energy budget after fire in boreal ecosystems of interior Alaska: An annual perspective, *J. Geophys. Res.*, *110*, D13101, doi:10.1029/2004JD005158.

Lyons, E. A., Y. F. Jin, and J. T. Randerson (2008), Changes in surface albedo after fire in boreal forest ecosystems of interior Alaska assessed using MODIS satellite observations, *J. Geophys. Res.*, *113*, G02012, doi:10.1029/2007JG000606.

Marshall, I. B., P. H. Schut, and M. Ballard (1999), A national ecological framework for Canada: Attribute data, report, Environ. Canada, Ottawa.

McGuire, A. D., et al. (2004), Land cover disturbances and feedbacks to the climate system in Canada and Alaska, in *Land Change Science*, edited by G. Gutman et al., pp. 139–161 pp., Springer, Dordrecht, Netherlands.

McMillan, A. M. S., and M. L. Goulden (2008), Age-dependent variation in the biophysical properties of boreal forests, *Global Biogeochem. Cycles*, *22*, GB2023, doi:10.1029/2007GB003038.

O'Halloran, T. L., et al. (2012), Radiative forcing of natural forest disturbances, *Global Change Biol.*, *18*(2), 555–565, doi:10.1111/j.1365-2486.2011.02577.x.

Price, D. T., and M. J. Apps (1995), The boreal forest transect case study : Global change effects on ecosystem processes and carbon dynamics in boreal Canada, *Water Air Soil Pollut.*, *82*(1-2), 203–214, doi:10.1007/BF01182834.

Randerson, J. T., et al. (2006), The impact of boreal forest fire on climate warming, *Science*, *314*(5802), 1130–1132, doi:10.1126/science.1132075.

Schaaf, C. B., et al. (2002), First operational BRDF, albedo nadir reflectance products from MODIS, *Remote Sens. Environ.*, *83*(1-2), 135–148, doi:10.1016/S0034-4257(02)00091-3.

Serbin, S. P., S. T. Gower, and D. E. Ahl (2009), Canopy dynamics and phenology of a boreal black spruce wildfire chronosequence, *Agric. For. Meteorol.*, *149*(1), 187–204, doi:10.1016/j.agrformet.2008.08.001.

Stocks, B. J., et al. (2003), Large forest fires in Canada, 1959–1997, *J. Geophys. Res.*, *108*(D1), 8149, doi:10.1029/2001JD000484.

Timoney, K. P., G. H. Laroi, and M. R. T. Dale (1993), Sub-Arctic forest-tundra vegetation gradients : The sigmoid wave hypothesis, *J. Veg. Sci.*, *4*(3), 387–394, doi:10.2307/3235597.

Turetsky, M. R., et al. (2011), Recent acceleration of biomass burning and carbon losses in Alaskan forests and peatlands, *Nat. Geosci.*, *4*(1), 27–31, doi:10.1038/ngeo1027.

Zhang, Y. C., W. B. Rossow, A. A. Lacis, V. Oinas, and M. I. Mishchenko (2004), Calculation of radiative fluxes from the surface to top of atmosphere based on ISCCP and other global data sets: Refinements of the radiative transfer model and the input data, *J. Geophys. Res.*, *109*, D19105, doi:10.1029/2003JD004457.